Influence of Synchronization Impairments on an Experimental TDOA/FDOA Localization System

Hugo Seuté, Cyrille Enderli, Jean-François Grandin, Ali Khenchaf, Jean-Christophe Cexus

Journal of Electrical Engineering 5 (2017) 1-9
doi: 10.17265/2328-2223/2017.01.001

Influence of Synchronization Impairments on an Experimental TDOA/FDOA Localization System

Hugo Seuté[1], Cyrille Enderli[1], Jean-François Grandin[1], Ali Khenchaf[2] and Jean-Christophe Cexus[2]

1. Thales Airborne Systems, 2 Avenue Gay Lussac, 78990 Elancourt, FRANCE

2. Lab-STICC, UMR CNRS 6285, ENSTA Bretagne, 2 Rue François Verny, 29806 Brest, FRANCE

Abstract: In Electronic Warfare, and more specifically in the domain of passive localization, accurate time synchronization between platforms is decisive, especially on systems relying on TDOA (time difference of arrival) and FDOA (frequency difference of arrival). This paper investigates this issue by presenting an analysis in terms of final localization performance of an experimental passive localization system based on off-the-shelf components. This system is detailed, as well as the methodology used to carry out the acquisition of real data. This experiment has been realized with two different kinds of clock. The results are analyzed by calculating the Allan deviation and time deviation. The choice of these metrics is explained and their properties are discussed in the scope of an airborne bi-platform passive localization context. Conclusions are drawn regarding the overall localization performance of the system.

Key words: Synchronization, Allan variance, time deviation, TDOA, FDOA, passive localization, USRP (universal software radio peripheral).

1. Introduction

Historically, most passive localization systems based on electromagnetic radiation have been developed in the context of EW (electronic warfare), and were denoted as ESM (electronic support measures). Various military applications have emerged, where ESM devices are mounted onboard different kinds of platforms: airborne [1], naval [2] or even spatial [3].

Passive localization systems use the properties of a signal received at different positions and/or dates in order to compute an estimate of the position of the radiating source. These systems differ from communication systems in that the source does not cooperate with the receiver, thus the waveform is unknown *a priori* and cannot be used to improve an estimator of the position of the source.

Traditionally, these localization systems have relied on interferometry to obtain AOA (angle of arrival) measurements in order to triangulate the position of the source. But these measurements only have an accuracy of a few degrees and the acquisition time can be long before the location is estimated with the desired accuracy. This is why other types of measurements have been introduced. Many modern techniques used in passive localization now rely on time and frequency based measurements on different platforms. For example, many techniques are based on the calculation of T/FDOA (time/frequency difference of arrival) [1-5], and scan-based localization techniques use the dates of interception of the main lobe of a rotating emitter [6]. Since the measurements depend on the time on two or more remote platforms, several clocks are needed. All clocks have imperfections which make them drift, yet a single time base must be maintained all along the measurement time, hence the need to synchronize the devices [5].

Synchronization can be done in practice by exchanging a signal in different configurations: one-way, two-ways, common view [7]. It is also possible to dispense with a sync signal if beacons of known positions can be seen by the receivers [8].

Corresponding author: Ali KHENCHAF, professor, research fields: radar, sea clutter, radar cross section, sea EM scattering, complex targets EM scattering, signal processing and remote sensing.

This article focuses on a system designed for combined TDOA/FDOA localization in a short-base airborne ESM context. This is a challenging scenario for a synchronized system because the measured time and frequency differences are small, thus the synchronization error must be kept as low as possible in order to have good precision [5]. In the scope of this article we will try to determine what performance in sync error we can expect in real-life situations via implementation and analysis of a full synchronization system, comprised of hardware (clocks, digital receivers) and software (delay estimation algorithm) processing. Then this will be translated in terms of localization error, in a simple scenario.

The paper is organized as follows: Section 2 presents some theoretical background on clock impairments and how to characterize sync error; Section 3 describes the methodology and the experimental process of the measurements which were carried out; in Section 4 the results for two different types of embedded clocks are shown and analyzed from an operational point of view; Section 5 establishes the link between sync error and localization performances; finally global conclusions and perspectives are presented in Section 6.

2. Timekeeping Issues

A clock can be modeled as a device producing a sine wave output of the form [9]:

$$V(t) = \big(V_0 + \epsilon(t)\big)\sin\big(2\pi f_0 t + \phi(t)\big) \quad (1)$$

where V_0 is nominal peak output voltage, $\epsilon(t)$ amplitude noise, f_0 nominal frequencyand $\phi(t)$ phase fluctuation (noise). In the case of time and frequency analysis, we can usually ignore the $\epsilon(t)$ term. From there we can identify two parameters of interest [9]:

Time fluctuation:

$$x(t) = \frac{\phi(t)}{2\pi f_0} \quad (2)$$

Fractional frequency, derived from the latter:

$$y(t) = \frac{dx(t)}{dt} = \frac{1}{2\pi f_0}\frac{d\phi(t)}{dt} \quad (3)$$

Due to the non-stationary nature of $\phi(t)$, these quantities cannot be analyzed through traditional statistics, the standard variance estimator will not converge as the number of samples increases [10]. In order to have a way to evaluate the amount of fluctuation of fractional frequency $y(t)$, the Allan variance $\sigma_y^2(\tau)$ was introduced [9, 11]. It measures the variance of the difference of two values of y spaced by a time τ. An efficient estimator for the Allan variance can be expressed in terms of time data:

$$\sigma_y^2(\tau) \approx \frac{1}{2(N-2m)\tau^2}\sum_{i=1}^{N-2m}(x_{i+2m} - 2x_{i+m} + x_i)^2 \quad (4)$$

where τ is the time horizon on which the variance is calculated, x_k the k^{th} sample of a dataset containing N values of $x(t)$ sampled every T_s, and $m = \tau/T_s$ the number of samples of $x(t)$ contained in the time horizon τ (m must be an integer such as $m \geq 1$).

Other types of variances similar to the Allan variance were developed, like the modified Allan variance, which is capable to distinguish between more types of noise [9, 12]. The expression of its estimate in terms of time data is:

$$Mod\ \sigma_y^2(\tau) \approx \frac{1}{2m^2\tau^2(N-3m+1)} \times \sum_{j=1}^{N-3m+1}\left[\sum_{i=j}^{j+m-1}(x_{i+2m} - 2x_{i+m} + x_i)\right]^2 \quad (5)$$

The time Allan variance is based on the modified (frequency) Allan variance and characterizes the time error of a clock [13]. It can be expressed as:

$$\sigma_x^2(\tau) = (\tau^2/3)\cdot Mod\ \sigma_y^2(\tau) \quad (6)$$

All the considerations stated above refer to the characterization of a single clock. But in practice it is not possible to measure the absolute fluctuations of a clock ($x(t)$ and $y(t)$) without having another clock to use as a time reference for t. Therefore $x(t)$ and $y(t)$ do not represent the absolute fluctuation of a single clock but the fluctuations of a clock relative to another reference clock. $x(t) = 0$ s and $y(t) = 0$ means that at a date t the two clocks are perfectly aligned with each other and their frequency is exactly the same.

$\sigma_x(\tau)$ can be interpreted as the standard deviation of the time error between the clocks considering an integration time of τ. For example, considering that the

time error is a white phase noise (such as in the simulation illustrated on Fig. 1a), we have $\sigma_x(\tau) \propto 1/\sqrt{\tau}$ [13] (as shown on Fig. 1b). It means that the lowest standard deviation of the error is attained when $\tau \to \infty$, so the synchronization process must apply a correction offset corresponding to the mean of as many values of $x(t)$ as possible.

On the contrary, if the time error can be modeled by a white frequency noise (like the simulation in Fig. 2a), we have $\sigma_x(\tau) \propto \sqrt{\tau}$ [13] (see Fig. 2b). In this situation, the lowest standard deviation is achieved when $\tau \to 0$ i.e. $T_s \to 0$. In this case, the best synchronization strategy is to sample $x(t)$ at the highest frequency and use the vector of time errors to correct the time base, without any averaging.

In the case of a complex noise model composed of the sum of different noise types (for example in Fig. 3, white phase noise and white frequency noise), the function $\sigma_x(\tau)$ may reach a minimum τ_0. Again, an example is given in Fig. 3. There, a good way to have a synchronized time base may be to compute the mean of $x(t)$ (which is sampled every T_{s0} with $T_{s0} \leq \tau_0$) on a sliding window of width τ_0 and use the series of these means as a correction.

Similarly, $\sigma_y(\tau)$ can be interpreted as the standard deviation of the relative frequency between the clocks, considering an integration time of τ. Its expression being directly linked to that of $\sigma_x(\tau)$, a representation of $\sigma_y(\tau)$ also reflects different types of noise: for white frequency noise, we would have $\sigma_y(\tau) \propto 1/\sqrt{\tau}$ and for random walk frequency noise $\sigma_y(\tau) \propto \sqrt{\tau}$. The calculation of $\sigma_y(\tau)$ also makes it possible to choose the best integration time τ in order to have the lowest value of $\sigma_y(\tau)$.

Now we will try to apply the same type of analysis and identify the noise type of real time error data that could have been obtained in an actual ESM system.

3. Methodology and Measurements

In this section will be described the experimental

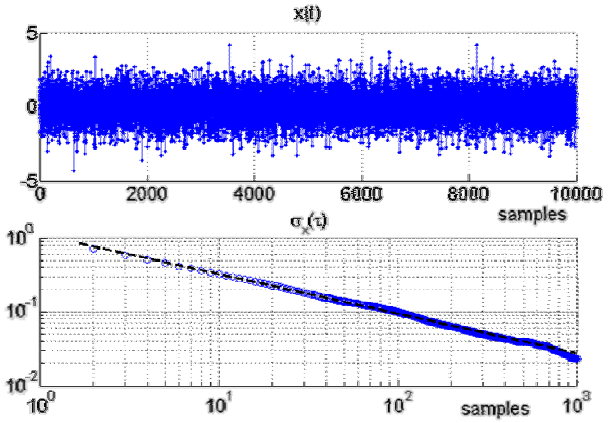

Fig. 1 Representation of time error as a function of time (Fig. 1a, *top*) and time deviation as a function of integration time (Fig. 1b, *bottom*) of a simulated white phase noise process.

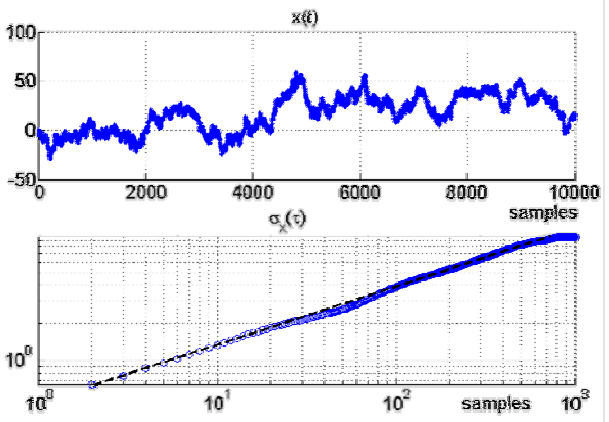

Fig. 2 Representation of time error as a function of time (Fig. 2a, *top*) and time deviation (Fig. 2b, *bottom*) of a simulated white frequency noise process.

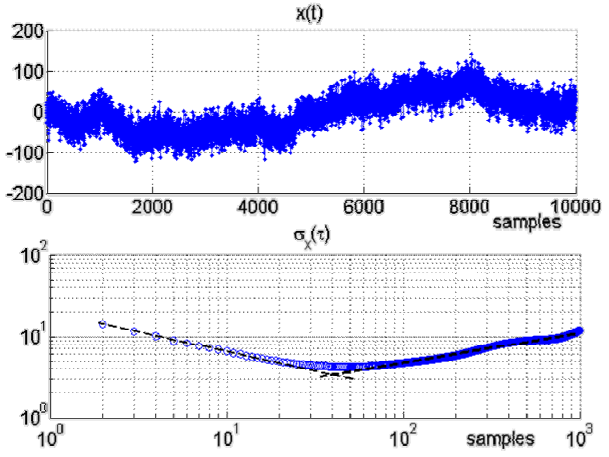

Fig. 3 Representation of time error as a function of time (Fig. 3a, *top*) and time deviation as a function of integration time (Fig. 3b, *bottom*) of a simulated noise process composed of both white phase noise and white frequency noise.

protocol used to acquire time fluctuation data on a passive bi-platform localization system. What we want to evaluate here is not just the performance (in terms of time error) of the clocks of the receivers, but the overall performance of a whole passive system, composed of two remote receivers, including their internal hardware and software processing, their clock and their synchronization protocol.

The receivers used for this experimental study are two SDR (software defined radio) platforms based on a USRP B210 (receiver #1) and a B200 (receiver #2) card, linked to a laptop computer to record the data. This setup was chosen because it allows quick development and experimentation tasks on radio frequencies from 70 MHz to 6 GHz, it is quite cheap and is available off-the-shelf. Experimental studies on TDOA have already been carried out on USRP devices such as Ref. [14] but they did not analyze thoroughly synchronization error.

Here, in order to have an accurate way to measure time error between two receivers, a synchronization system has been developed (Fig. 4), based on the emission of a periodic sync signal. The emitter of this signal is actually collocated with receiver #1, inside the B210 card. In this experiment two platforms are located close to each other so that the propagation delay can be neglected. In the case of a real system this delay cannot be neglected, but it can be estimated and cancelled if the platform positions are known [15].

The sync signal is used for two things:

- When it is detected (via a simple threshold detector on the signal's band), the receivers start recording a fixed number of samples into a time stamped file. This avoids to record permanently and to have a huge amount of data to process in the following steps.
- The complex envelopes of the sync signals recorded by the two receivers are processed to accurately obtain the time difference between them.

This delay estimation process is described in Refs. [15] and [16]. It is done in four steps, as illustrated on Fig. 5: First the complex envelopes are cross-correlated,

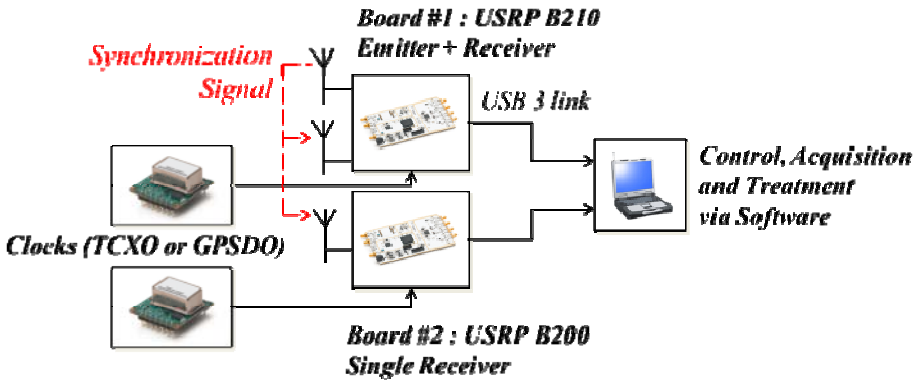

Fig. 4 Diagram of the experimental set-up.

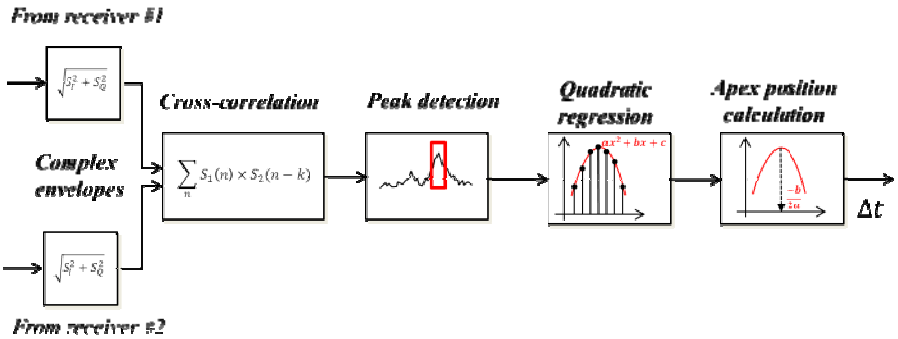

Fig. 5 Diagram of the delay estimation process.

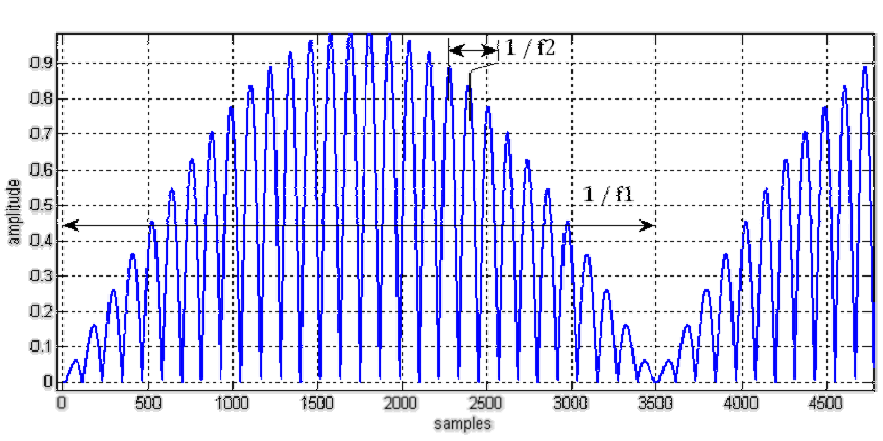

Fig. 6 A representation of the envelope of the sync signal with $f_1 = 1$ kHz and $f_2 = 30$ kHz, sampled every $T = 143$ ns.

Table 1 Values of the parameters of interest.

P.	Value	Description
T_s	10 s	Sync signal period of emission
T	143 ns	Sampling period
D_r	200 ms	Duration of the record of the sync signal
f_1	1 kHz	Frequency of the first modulation of the sync signal
f_2	3 MHz	Frequency of the second modulation of the sync signal
f_{LO}	5 GHz	Nominal frequency of the local oscillators on the receivers and emitter

next the points around the main peak of the cross-correlation function are selected, these points are then interpolated by a parabola, and finally the apex of the parabola is computed, which corresponds to the final estimate of the delay between the two signals. In our experiment, the two receivers are situated right next to each other so the difference of path of the sync signal between the two platforms can be neglected. Thus the value at the output of the delay estimation chain directly corresponds to an estimate $\hat{x}(t)$ of $x(t)$ the time error between each receiver.

Due to these different purposes, there are different requirements on this signal:

• When cross-correlation is computed from the envelope of the signals contained in the two files, the cross-correlation peak must be unambiguous: there must be a single peak which occurs inside an interval of possible delays. Indeed, if the sync signal is periodic with a short period—shorter than the maximum time offset expected between the two records—there will be several cross-correlation peaks that could correspond to a consistent delay estimation.

• This cross-correlation peak needs to be narrow to improve the accuracy of delay estimation. In Ref. [16] it is stated that the standard deviation of the time offset estimation is proportional to $1/\beta$, where β is the "root mean square radian frequency" of the cross-correlated signals, defined by

$$\beta = 2\pi \left[\frac{\int_{-\infty}^{\infty} f^2 W_s(f) df}{\int_{-\infty}^{\infty} W_s(f) df} \right]^{1/2} \quad (7)$$

where $W_s(f)$ is the signal power density spectrum. Hence the synchronization signal needs to have high frequency components to provide accurate delay estimation.

A signal complying with these requirements has been chosen arbitrarily (represented on Fig. 6). It is composed of a carrier modulated in amplitude by a low and a high frequency signal (satisfying respectively the first and second requirement).

$$s(t) = \sin(2\pi f_1 t) \sin(2\pi f_2 t) e^{j2\pi f_{LO} t} \quad (8)$$

where f_1 and f_2 are the frequencies of the modulated signals and f_{LO} is the carrier frequency.

The settings used during the measurements are grouped on Table 1.

Now that we have a system capable of giving time fluctuations measurements between two receivers, the next step is to produce these data in conditions that are consistent with operational contexts.

4. Measurement Analysis

Two experiments have been carried out, each featuring a different type of clock (A or B). The same clock type is mounted on both receivers on an experiment. Clocks type A are TCXO (temperature compensated crystal oscillator) and clocks type B are GPSDO (GPS disciplined oscillator), which are clocks actually based on the same TCXO but joined to an internal control loop using the 1-PPS (pulse per second) signal from a GPS receiver as a reference.

Fig. 7 represents two series of time fluctuation measurements $\hat{x}(t)$ between the two platforms, with the reception system fitted either with clocks type A or clocks type B. Fig. 8 shows the time deviation computed from the latter measurements using Eqs. (4) and (5). Fig. 9 shows the Allan deviation from the same data, using (X). The acquisition time for these experiments was 1 hour. The Allan deviation plot is limited to 360 s, because values of $\sigma_{\hat{x}}(\tau)$ and $\sigma_{\hat{y}}(\tau)$ for τ close to acquisition time may not be relevant (less samples are averaged, the confidence interval is too large). In other applications, longer acquisition time is often used to analyze the long term behavior of a clock, but in our context of airborne ESM, it appears unlikely that the synchronization period of the system exceeds several minutes.

What we can see from the time deviation plot (Fig. 8) is that the free running clocks (type A) have good short term time stability but when it is left unsynchronized for a long time, time deviation $\sigma_{\hat{x}}(\tau)$ increases proportionally to $\tau^{3/2}$, which is characteristic of a random walk frequency modulation noise [13]. Type A clocks reach a minimum time deviation of 2.5 ns. This minimum is reached when $\hat{x}(t)$ is averaged during a period $\tau_0 = 40$ s (4 measurements).

Clocks type B have a worse short term time stability,

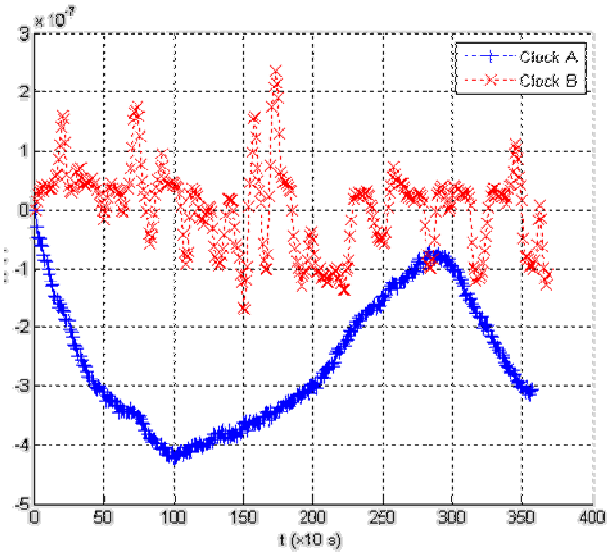

Fig. 7 Measured time error $\hat{x}(t)$ between platforms, for the two experiments.

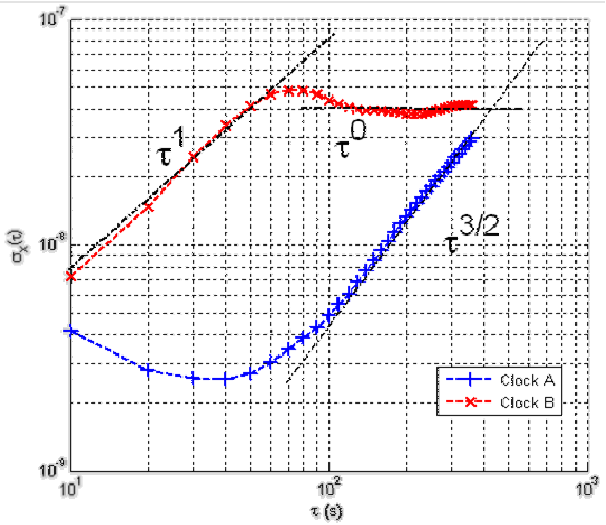

Fig. 8 Experimental time deviation $\sigma_{\hat{x}}(\tau)$ between platforms.

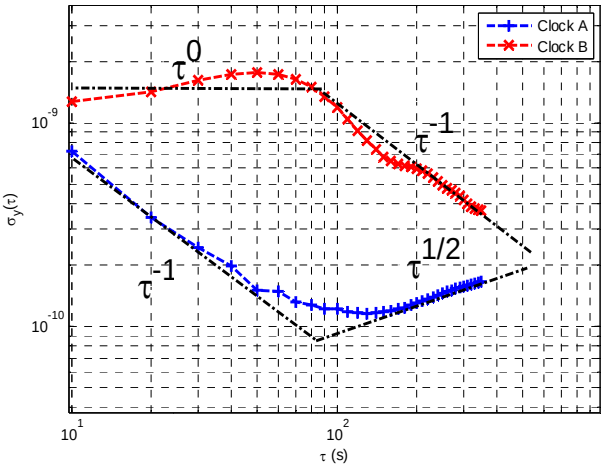

Fig. 9 Experimental Allan deviation $\sigma_{\hat{y}}(\tau)$ between platforms.

probably because of an internal control loop which may introduce some high frequency noise in the system. Time deviation increases proportionally to τ, which is representative of a flicker frequency modulation noise [13]. But then it becomes constant (i.e. $x(t)$ is affected by flicker phase modulation noise) after 60 seconds, showing a time deviation of $\sigma_{\hat{x}}\,(\tau > 50\text{ s}) \approx 40\text{ ns}$, which is coherent with time accuracy for a GPS signal [17].

The Allan deviation plot (Fig. 9) gives information about the fluctuations of fractional frequency between the platforms. For clocks type A the Allan deviation decreases proportionally to $1/\tau$ until it reaches a minimum of 1.2×10^{-10} for an integration time of $\tau_0 = 130$ s. It is interesting to note that the integration time minimizing the Allan deviation is different from that minimizing time deviation. For the other types of clocks (type B), the Allan deviation stays approximately constant at 1.5×10^{-9} until $\tau = 50$ s then it starts decreasing proportionally to $1/\tau$.

If we extrapolate the results, we see that the minimum time deviation would be achieved by using clock A for $\tau < 430$ s and clock B otherwise. For fractional frequency deviation (Allan deviation), clock A appears to be better for $\tau < 600$ s. So if the synchronization period T_s is high (or even infinite: no sync signal exchanged), a GPSDO appears to be the best choice. Typically, this case can happen if the datalink providing synchronization capabilities to the receivers is restricted or unavailable (for stealth purposes or because of jamming). On the contrary, if a short period synchronization signal is available, a standard TCXO seems to be a better option.

5. Localization Performances

In the previous sections we have shown that with the considered synchronization system, using TCXOs and by exchanging a synchronization signal every 10 sec, with the optimal integration time it was possible to attain a time deviation of $\sigma_{\hat{x}} = 2.5$ ns and a fractional frequency deviation of $\sigma_{\hat{y}} = 1.2 \times 10^{-10}$. For a TDOA/FDOA system, the overall standard deviations of the measurements errors can be modeled by:

$$\sigma_{TDOA} = \sqrt{\sigma_{\hat{x}}(\tau)^2 + \sigma_t^2} \tag{9}$$

$$\sigma_{FDOA} = \sqrt{f_0\sigma_{\hat{y}}(\tau)^2 + \sigma_f^2} \tag{10}$$

where σ_t^2 and σ_f^2 are the variances of the instrumental error for time and frequency measurements, considered constant over time and independent from other synchronization errors. Considering that these instrumental errors are null, we obtain a lower bound on TDOA and FDOA errors. This lower bound represents the case where errors are only due to the imperfect synchronization of the system. We are now looking for how to represent this lower bound in terms of localization performance for a simple scenario.

This scenario features two mobile receivers s_1 and s_2 following each other at speed v and intercepting RF emissions from a target m located on their side. The receivers are separated by a distance a and the source is at a distance d away from the center of the base (Fig. 10).

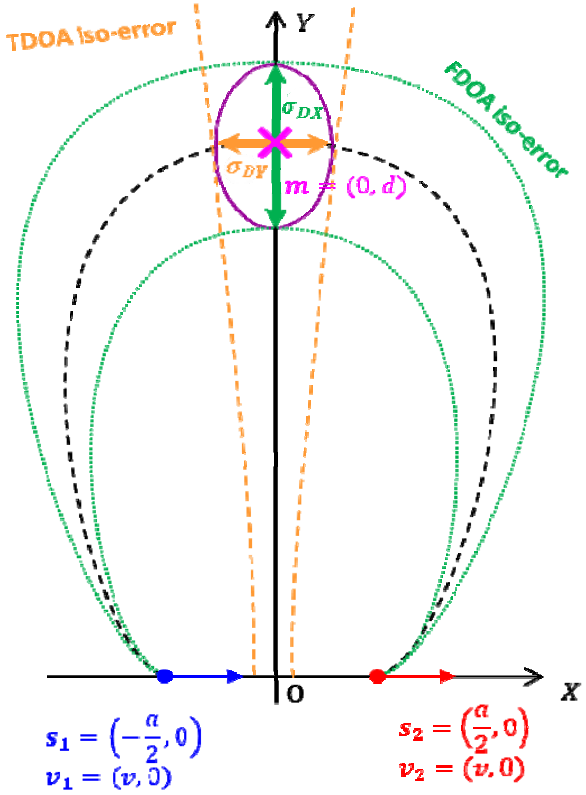

Fig. 10 Geometry of the scenario.

Under the hypothesis that $d \gg a$ (the base is short relative to the distance to the source) which is realistic in an airborne context, it is possible to obtain easily the CRLB (Cramér-Rao lower bound) of a position estimator of m [5]: its covariance matrix can be expressed as $\Sigma_{\hat{m}} = [\sigma_{DX}^2\ 0\ ;0\ \sigma_{DY}^2]$ with:

$$\sigma_{DX} = \sigma_{\hat{x}} \frac{cd}{a}, \sigma_{DY} = \sigma_{\hat{y}} \frac{cd^2}{av} \quad (11)$$

Considering $d = 50\,\text{km}$, $a = 1\,\text{km}$ and $v = 300\,\text{m/s}$, the lower bound of a position estimator considering synchronization errors only is: $\sigma_{DX} = 38\,\text{m}$, $\sigma_{DY} = 300\,\text{m}$. We remark that FDOA localization is more demanding in term of synchronization accuracy.

6. Conclusion

One of the objectives of this paper was to point out that the tools developed in frequency analysis (and more particularly the Allan deviation and time deviation) are very useful to characterize the performances of distributed passive localization systems. These tools help understand the operational impact of technological decisions such as the choices concerning the type of oscillator or the synchronization period of the data link.

The main objective was to describe the influence of a realistic synchronization scheme on the output localization performance. In order to attain this objective, a simple but realistic bi-platform system has been set up and time error data have been generated using two different sets of clock. Time and Allan deviations have been computed from these data, providing estimates of synchronization performance for the optimal integration time. These time and frequency performances were used to compute a lower bound for a localization estimator, in a simple yet relevant scenario. In the end, for the case we studied it appeared that the limiting factor was the accuracy in term of fractional frequency stability.

Further work is needed to take into account the platform position error when the differential propagation time of the sync signal cannot be neglected and must be estimated. Moreover, in this paper we only focused on time error noise, but the same principles could be extended to characterize complicated noise processes that can be present in other kinds of sensors, such as IMU (inertial measurements units).

References

[1] Arena, L., and Orlando, D. 2014. "Passive Location Developments in Elettronica SpA: System Applications." *2014 Tyrrhenian International Workshop on Digital Communications—Enhanced Surveillance of Aircraft and Vehicles (TIWDC/ESAV)*, 130-4.

[2] Wooller, D. 1985. "System Considerations for Naval ESM." In *IEE Proceedings of Communications, Radar and Signal Processing, F* 132 (4): 212-4.

[3] Yang, Z. B., Wang, L., Chen, P. Q., and Lu, A. N. 2013. "Passive Satellite Localization Using TDOA/FDOA/AOA Measurements." In *Proceedings of Conference Anthology, IEEE*, China, 1-5.

[4] Musicki, D., and Koch, W. 2008. "Geolocation Using TDOA and FDOA Measurements." *2008 11th International Conference on Information Fusion,* 1-8.

[5] Seute, H., Grandin, J.-F., Enderli, C., Khenchaf, A., and Cexus, J.-C. 2015. "Why Synchronization Is a Key Issue in Modern Electronic Support Measures." *2015 16th International on Radar Symposium (IRS),* 794-9.

[6] Hmam, H. 2007. "Scan-Based Emitter Passive Localization." *IEEE Transactions on Aerospace and Electronic Systems* 43 (1): 36-54.

[7] Cheng, L., Hailes, S., and Wilson, A. 2010. "Towards Precise Synchronisation in Wireless Sensor Networks." *2010 IEEE/IFIP 8th International Conference on Embedded and Ubiquitous Computing (EUC)*, 208-15.

[8] Pelant, M., and Stejskal, V. 2011. "Multilateration System Time Synchronization via Over-determination of TDOA Measurements." *2011 Tyrrhenian International Workshop on Digital Communications—Enhanced Surveillance of Aircraft and Vehicles (TIWDC/ESAV)*, 179-83.

[9] IEEE. 2009. "Standard Definitions of Physical Quantities for Fundamental Frequency and Time Metrology—Random Instabilities—Redline." In *Proceedings of IEEE Std. 1139-2008 (Revision of IEEE Std. 1139-1999)—Redline*, 1-51.

[10] Allan, D. W. 1987. "Should the Classical Variance Be Used as a Basic Measure in Standards Metrology?" *IEEE Transactions on Instrumentation and Measurement* IM-36 (2): 646-54.

[11] Allan, D. W. 1966. "Statistics of Atomic Frequency Standards." In *Proceedings of the IEEE* 54 (2): 221-30.

[12] Allan, D.W., and Barnes, J. A. 1981. "A Modified 'Allan Variance' with Increased Oscillator Characterization Ability." In *Thirty Fifth Annual Frequency Control Symposium,* 470-5.

[13] Allan, D. W., Weiss, M. A., and Jespersen, J. L. 1991. "A Frequency-Domain View of Time-Domain Characterization of Clocks and Time and Frequency Distribution Systems." In *Proceedings of the 45th Annual Symposium on Frequency Control,* 667-78.

[14] Seong, H. C., Sang, Rae, Y., Heon, H. C., Chansik, P., and Sang, J. L. 2012. "A Design of Synchronization Method for TDOA-Based Positioning System." In *Proceedings of 2012 12th International Conference on Control, Automation and Systems (ICCAS),* 1373-5.

[15] Seute, H., Grandin, J.-F., Enderli, C., Khenchaf, A., and Cexus, J.-C. 2016. "Experimental Measurement of Time Difference of Arrival." In *Proceedings of 17th International on Radar Symposium (IRS),* 1-4.

[16] Stein, S. 1981. "Algorithms for Ambiguity Function Processing." *IEEE Transactions on Acoustics, Speech and Signal Processing* 29 (3): 588-99.

[17] GPSDO Datasheet, Ettus Research, May 2014.